Water Resources Research

RESEARCH ARTICLE
10.1029/2019WR026083

A New Framework for Exploring Process Controls of Flow Duration Curves

Saba Ghotbi[1], Dingbao Wang[1], Arvind Singh[1], Günter Blöschl[2], and Murugesu Sivapalan[3,4]

[1]Department of Civil, Environmental, and Construction Engineering, University of Central Florida, Orlando, FL, USA, [2]Institute of Hydraulic Engineering and Water Resources Management, Technische Universität Wien, Vienna, Austria, [3]Department of Civil and Environmental Engineering, University of Illinois at Urbana-Champaign, Urbana, IL, USA, [4]Department of Geography and Geographic Information Science, University of Illinois at Urbana-Champaign, Urbana, IL, USA

Key Points:
- A new framework is proposed for exploring process controls of flow duration curves (FDC), which involves separating total streamflow into its fast and slow components
- The FDC of total streamflow can be constructed by combining FDCs of fast flow and slow flow components and a measure of their dependence
- The dependence between fast flow and slow flow is captured by a copula model and shows regional patterns

Correspondence to:
D. Wang,
dingbao.wang@ucf.edu

Citation:
Ghotbi, S., Wang, D., Singh, A., Blöschl, G., & Sivapalan, M. (2020). A new framework for exploring process controls of flow duration curves. *Water Resources Research*, *56*, e2019WR026083. https://doi.org/10.1029/2019WR026083

Received 2 AUG 2019
Accepted 3 JAN 2020
Accepted article online 05 JAN 2020

Abstract The flow duration curve (FDC) is effectively the cumulative distribution function of streamflow. For a long time, hydrologists have sought deeper understanding of the process controls on the shape of FDC, which has been a challenge due to contrasting processes controlling the fast flow and slow flow components of streamflow and their interactions. In this paper, we outline a new framework for exploring the process controls of the FDC, which involves studying fast and slow flow components of FDC separately and combining them statistically, explicitly accounting for their dependence. We illustrate the potential of the framework by constructing empirical fast flow duration (FFDC) and slow flow duration (SFDC) curves from the flow components obtained by traditional baseflow separation. Streamflow time series data from 245 MOPEX catchments across the continental United States are used. The dependence of FFDC and SFDC components is captured by the Gumbel copula, the strength of which varies regionally. In catchments where FFDC and SFDC are independent, FDC can be approximated by a simple convolution of FFDC and SFDC. The proposed conceptual framework opens the way for future modeling studies to explore process controls of fast and slow components of streamflow separately, their dependence, and their relative contributions to the shape of the FDC.

1. Introduction

The flow duration curve (FDC) is an important signature of a catchment's rainfall-runoff response (Vogel & Fennessey, 1994). It reflects the cumulative distribution function of streamflow (Smakhtin, 2001; Vogel & Fennessey, 1994). The FDC has a long history of applications in water resources planning and management (Dingman, 1981; Vogel & Fennessey, 1995), such as the assessment of hydropower potential (Castellarin et al., 2013), flood and low-flow analysis (Smakhtin, 2001), hydrologic effects of afforestation (Lane et al., 2005), sedimentation in rivers (Vogel & Fennessey, 1995), water quality management (Morrison & Bonta, 2008; Searcy, 1959), and determination of environmental flow standards for protecting aquatic habitats and ecosystem health (Olden & Poff, 2003; Poff et al., 1997).

Two types of FDCs have been defined in the literature, including the period-of-record flow duration curve (PoR-FDC), and annual flow duration curve (AFDC) (Castellarin et al., 2004; Searcy, 1959; Vogel & Fennessey, 1994, 1995). The PoR-FDC is computed based on the entire period of streamflow record thus representing the long-term, steady-state streamflow distribution; whereas, AFDC is computed based on the streamflow during a single year, and when analyzed separately for several years of the total record, this will be able to capture the interannual variability of intraannual streamflow variability. In this paper, PoR-FDC is the focus of the research.

The FDC of a catchment is controlled by climate, soil, topography, geology, vegetation, and human activities (Castellarin et al., 2013; Cheng et al., 2012). Identification of the physical characteristics that control the FDC is an important step toward predicting FDCs in ungauged catchments and toward predicting changes in the future under land use and/or climate changes. The climatic and physiographic controls on the shape of FDCs have been extensively investigated for the purpose of regionalization (Mohamoud, 2008; Singh, 1971). For example, Searcy (1959) highlighted the effect of catchment geology on FDCs, showing that the lower flow part of the curve is mainly controlled by catchment geology. Best et al. (2003) showed that the median flow and the fraction of zero flows are affected by vegetation type and climate. Yokoo and

Sivapalan (2011) investigated the sensitivity of FDCs to soil type and climatic seasonality and found that in the case of out-of-phase seasonality and well-drained soils, the FDCs tend to be ephemeral. Ye et al. (2012) and Yaeger et al. (2012) investigated the regional patterns of FDCs across continental United States and found that the dominant controlling factors on the FDCs vary regionally.

Both statistical and process-based approaches have been used for estimating FDCs and for understanding their climatic and landscape controls. Statistical methods rely on fitting a statistical distribution function to many observed FDCs in gauged sites in a region and then building regional regression relationships between the fitted parameters of the distribution and catchment properties (Castellarin et al., 2004, 2007; Li et al., 2010; Over et al., 2018; Singh et al., 2001; Vogel & Fennessey, 1994). For example, Castellarin et al. (2004, 2007) related the parameters of an index flow stochastic model fitted to the FDCs to the geomorphoclimatic characteristics of catchments (Castellarin et al., 2007). Likewise, Mohamoud (2008) showed that soil texture and depth are two strong descriptors for predicting FDCs in ungauged catchments.

The statistical methods outlined above do not explicitly address the process controls of FDC, which tends to make the resulting estimates of the FDC less reliable when the study catchments are outside the study regions and time periods within which the statistical relationships have been developed (Castellarin et al., 2013). For this reason, for a long time, hydrologists have aspired to develop process-based understanding of the climatic and landscape controls of the FDC. Past studies in this line of research have adopted a derived distribution approach by combining stochastic descriptions of rainfall inputs with a deterministic description of the rainfall-runoff transformation. For example, Botter, Porporato, Daly, et al. (2007) and Botter, Porporato, Rodriguez-Iturbe, and Rinaldo (2007) studied process controls of the FDC using a stochastic conceptual model of the catchment system, consisting of a sequence of rainfall events modeled as a Poisson process and a lumped, deterministic water balance model. The initial focus was on analytical derivations to make it easier to understand the process controls of the FDC. This stochastic model was extended later by using a nonlinear storage-discharge relationship in the underlying water balance model (Botter et al., 2009). Because of the assumption of Poisson arrivals with constant parameters, the derived distribution approach of Botter, Porporato, Daly, et al. (2007) and Botter, Porporato, Rodriguez-Iturbe, & Rinaldo (2007, 2009) was limited to catchments with a dominant wet season, and was inapplicable to predictions of FDCs in locations which experience strong seasonality. The focus on total streamflow also meant the model could not separately accommodate differences in relative contributions of fast (surface) and slow (subsurface) to total streamflow. Müller et al. (2014) extended the derived distribution approach of Botter, Porporato, Rodriguez-Iturbe, and Rinaldo (2007) to seasonally dry climates by modeling streamflow during the wet season using the Botter, Porporato, Rodriguez-Iturbe, and Rinaldo (2007) model and streamflow during the dry season using a deterministic recession curve with a stochastic initial condition. While these represent significant progress in the process-based, derived distribution approach, rainfall-runoff processes in real catchments around the world exhibit much more complexity and regional heterogeneity than has been assumed in these early efforts (Blöschl et al., 2013; Yaeger et al., 2012). There is therefore a clear need for approaches or conceptual frameworks that can be used to study process controls of the FDC more generally.

The challenge of modeling FDCs and understanding the process controls of the shape of FDC is due to the fact that total streamflow is a combination of catchment hydrologic responses operating at multiple time scales (Beckers & Alila, 2004; Blöschl et al., 2013; Yokoo & Sivapalan, 2011). For simplicity, as a first step, streamflow can be separated into two time scales: fast flow representing surface runoff and slow flow representing subsurface streamflow and groundwater flow. Both fast flow and slow flow can be further disaggregated into three parts: high flow, midrange flow, and low flow. Figure 1a shows the schematic partitioning of daily streamflow into separate fast flow and slow flow time series. Processes controlling fast flows are surface runoff generation (e.g., infiltration and/or saturation excess runoff generation) and surface runoff routing. The variability of fast flows is governed by stochastic characteristics of the sequences of storm events experienced by the catchment and the properties of surface soils and topography. Processes controlling slow flows include subsurface flow and groundwater discharge. The variability of slow flows strongly reflects climate seasonality and the underlying geology of the aquifer system and may yet retain aspects of storminess not lost through the filtering effect of unsaturated zone surface soils. There is also feedback between the surface and subsurface (groundwater) processes in the form of groundwater recharge and the influence of groundwater levels on antecedent soil moisture of surface soils. These distinct differences between process controls of fast and slow flows present an opportunity to model fast and slow flows and their interdependence separately, explore their

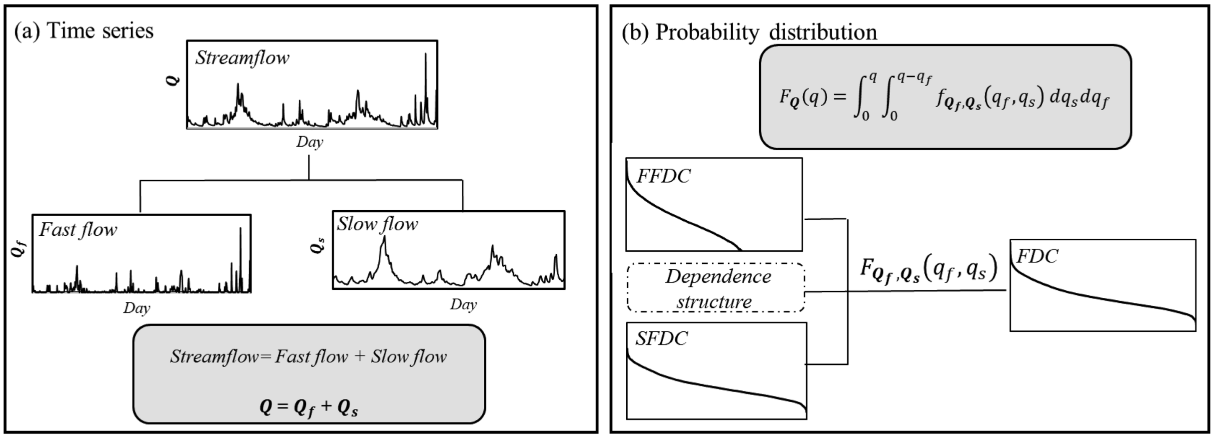

Figure 1. The schematic illustration of the proposed framework for modeling flow duration curve (FDC): (a) Streamflow time series is decomposed into fast flow time series and slow flow time series; and (b) FDC is computed as the sum of fast flow and slow flow considering the dependence between them.

process controls independently, and later combine them to model the FDC of total streamflow. The FDC of total streamflow can thus be seen as a statistical summation of a fast flow duration curve (FFDC) and a slow flow duration curve (SFDC) (Yokoo & Sivapalan, 2011), with appropriate adjustments made for their interdependence.

Based on the above arguments, in this paper we present a new conceptual framework for exploring process controls of FDC. This framework includes three components: (1) the probability distribution of fast flow; (2) the probability distribution of slow flow; and (3) a method for constructing FDC of total streamflow by combining FFDC and SFDC, accounting for the dependency between fast and slow flows. We illustrate the framework by applying it to catchments across the continental United States. As a first step, the fast and slow flow components are estimated empirically from observed total streamflow using an empirical baseflow separation approach. This allows us to construct the flow duration curves of fast and slow flow components of streamflow (i.e., FFDC and SFDC, respectively) separately, and combine the FFDCs and SFDCs to construct FDC of total streamflow, accounting for their dependency.

2. Framework for Process-Based Exploration of FDC

The FDC used in hydrology is the complementary cumulative distribution function of streamflow, usually constructed from daily streamflow. Daily streamflow is considered as the sum of daily fast and slow flows:

$$\boldsymbol{Q} = \boldsymbol{Q_f} + \boldsymbol{Q_s} \tag{1}$$

where $\boldsymbol{Q}$, $\boldsymbol{Q_f}$, and $\boldsymbol{Q_s}$ are random variables representing daily streamflow, fast flow, and slow flow, respectively. Given equation (1) and considering the joint probability density function of fast flow and slow flow, the cumulative distribution function (CDF) for $\boldsymbol{Q}$ can be expressed as

$$F_{\boldsymbol{Q}}(q) = P(\boldsymbol{Q_f} + \boldsymbol{Q_s} \leq q) = \int_0^q \int_0^{q-q_f} f_{\boldsymbol{Q}_f,\boldsymbol{Q}_s}\left(q_f, q_s\right) \mathrm{d}q_s \mathrm{d}q_f \tag{2}$$

where $F_{\boldsymbol{Q}}(q)$ is the CDF of streamflow, and $f_{\boldsymbol{Q}_f,\boldsymbol{Q}_s}\left(q_f, q_s\right)$ is the joint probability density function of fast flow and slow flow. The probability density function (PDF) for streamflow can be obtained by taking the derivative of both sides of equation (2):

$$f_{\boldsymbol{Q}}(q) = \frac{d}{dq}\left[\int_0^q \int_0^{q-q_f} f_{\boldsymbol{Q}_f,\boldsymbol{Q}_s}\left(q_f, q_s\right) \mathrm{d}q_s \mathrm{d}q_f\right] \tag{3}$$

10.1029/2019WR026083

By applying the Leibniz integral rule to the outer integral on the right-hand side of equation (3), one nonzero term is retained as follows:

$$f_{Q}(q) = \int_{0}^{q} \frac{d}{dq}\left[\int_{0}^{q-q_f} f_{Q_f,Q_s}\left(q_f, q_s\right) \mathrm{d}q_s\right]\mathrm{d}q_f \tag{4}$$

Applying the Leibniz integral rule again to the inner integral on the right-hand side of equation (4), the PDF for streamflow is obtained as

$$f_{Q}(q) = \int_{0}^{q} f_{Q_f,Q_s}\left(q_f, q-q_f\right) \mathrm{d}q_f \tag{5}$$

The joint distribution of fast and slow flows is used here since the fast flow and slow flow in catchments may not be statistically independent. In the example of Figure 1a, both fast flow and slow flow are higher in the wet season compared to those in the dry season. As a special case, when fast flow and slow flow are independent, equation (5) simplifies to a convolution of the PDFs of fast flow and slow flow. Denoting the PDF for fast flow as $f_{Q_f}\left(q_f\right)$ and the PDF for slow flow as $f_{Q_s}(q_s)$, the PDF for $\boldsymbol{Q}$, that is, $f_{Q}(q)$, in the case of their statistical independence, is obtained as

$$f_{Q}(q) = \int_{0}^{q} f_{Q_s}\left(q-q_f\right) f_{Q_f}\left(q_f\right) \mathrm{d}q_f \tag{6}$$

3. Illustration of the Framework

In this paper, the proposed framework is illustrated on the MOPEX catchments (Duan et al., 2006). The daily streamflow data during 1948 to 1977 from 305 catchments with minimum human interferences (Wang & Hejazi, 2011) are selected for analysis. The drainage area of the study catchments varies from 180 to 9,500 km^2. The average elevation ranges from 35 to 2,700 m above the mean sea level, and the average land surface slope varies from 2% to 50%. The mean annual precipitation ranges from 350 to 2,800 mm, and the climatic aridity index, defined as the ratio of mean annual potential evaporation to mean annual precipitation, ranges from 0.25 to 4.11. Therefore, the study catchments are located in both humid and arid regions.

3.1. PDFs for Fast and Slow Flows

Since the focus of this paper is to illustrate a general framework for modeling FDC by combining FFDC and SFDC, as a first step, the fast flow and slow flow components of streamflow are estimated here from observed total streamflow using empirical baseflow separation method. Several methods have been proposed for separating streamflow into fast flow and slow flow components (Eckhardt, 2005; Horton, 1933; Lyne & Hollick, 1979). Neff et al. (2005) compared six different baseflow separation methods for developing a regression model to estimate baseflow and the baseflow index (BFI), defined as the ratio between long-term averaged baseflow and total runoff.

In the present study, two methods, that is, nonlinear recession analysis and a recursive digital filter, are used for baseflow separation. The separation method based on nonlinear recession analysis, which is a more process-based method, assumes a nonlinear storage-outflow relationship for modeling the recession limbs (Wittenberg, 1999; Wittenberg et al., 2019; Wittenberg & Sivapalan, 1999). The recursive digital filter method, referred to as filter-based method, separates the slow flow signals from fast flow signals to extract the slow flow hydrograph (Eckhardt, 2005). The details of the process-based and filter-based separation methods are presented in Appendix A.

By applying the baseflow separation methods to daily streamflow, the FFDC is constructed from daily fast flow, and the SFDC is constructed from daily slow flow (Yokoo & Sivapalan, 2011), as demonstrated in Figure 1b.

3.2. Quantifying the Dependence of Fast and Slow Flows Using Copula

For catchments where fast flow and slow flow are dependent, the joint CDF of fast flow and slow flow can be quantified by a copula function (Nelsen, 2007; Sklar, 1959):

$$F_{\boldsymbol{Q}_f,\boldsymbol{Q}_s}\left(q_f,q_s\right)=C\left(F_{\boldsymbol{Q}_f}\left(q_f\right),F_{\boldsymbol{Q}_s}(q_s)\right) \tag{7}$$

where $F_{\boldsymbol{Q}_f,\boldsymbol{Q}_s}\left(q_f,q_s\right)$ is the joint CDF of fast flow and slow flow; $F_{\boldsymbol{Q}_f}\left(q_f\right)$ is the CDF of fast flow; $F_{\boldsymbol{Q}_s}(q_s)$ is the CDF of slow flow; and C is a copula function which quantifies the joint CDF of fast flow and slow flow as a function of $F_{\boldsymbol{Q}_f}\left(q_f\right)$ and $F_{\boldsymbol{Q}_s}(q_s)$. Copulas have been applied for characterizing complex hydrological events such as floods through a small number of dependent variables such as flood peak, volume, and duration (Favre et al., 2004; Grimaldi & Serinaldi, 2006; Salvadori & De Michele, 2004; Szolgay et al., 2016; Zhang & Singh, 2007). Kao and Govindaraju (2008) applied a trivariate copula to characterize the temporal distribution of extreme rainfall. Shiau (2006) utilized copulas to characterize hydrological drought by modeling the joint distribution of drought duration and severity.

The first step in modeling the joint distribution through a copula function is the choice of the copula that explains the association between random variables. Archimedean is a widely used class of copulas with several simple closed form functions (Genest & MacKay, 1986). The Gumbel, Clayton, and Frank copulas are three well-known Archimedean copulas applied in hydrology and use one parameter (θ) to capture the dependency (Salvadori & De Michele, 2004; Zhang & Singh, 2006). Table 1 shows the functional forms of the three copulas as a function of $F_{\boldsymbol{Q}_f}\left(q_f\right)$ and $F_{\boldsymbol{Q}_s}(q_s)$. In each form of the copulas, θ accounts for the association between fast flow and slow flow; the range of θ values is also shown in Table 1. From Table 1, it can be seen that the Gumbel and Clayton copulas cannot account for the negative dependence, in which case the Frank copula is applied. For example, for the Gumbel copula, $\theta = 1$ represents the independence condition and $\theta > 1$ represents positive dependence. The degree of association between fast flow and slow flow can be quantified by Kendall's τ, which can be computed by the following equation (Schweizer & Wolff, 1981):

$$\tau=\frac{2}{n(n-1)}\sum_{i=1}^{n-1}\sum_{j=i+1}^{n}\operatorname{sgn}\left[\left(Q_{f,i}-Q_{f,j}\right)\left(Q_{s,i}-Q_{s,j}\right)\right] \tag{8}$$

where $Q_{f,i}$ and $Q_{s,i}$ are fast flow and slow flow on the ith day, respectively; $Q_{f,j}$ and $Q_{s,j}$ are fast flow and slow flow on the jth day, respectively; n is the total number of days; and sgn represents the sign function. The relationships between θ and Kendall's τ for the three copulas are shown in Table 1. Therefore, θ for each copula can be estimated by the computed Kendall's τ.

Several tests have been developed to assess the goodness-of-fit of a copula (Chen et al., 2004; Fermanian, 2005; Genest et al., 2006). All tests attempt to examine the hypothesis that a specific copula defines the dependence structure of a multivariate distribution appropriately. The Cramér-von Mises test is powerful to compare the distance between the empirical distribution and the copula-based distribution for a specific copula (Genest & Rémillard, 2008). The details of the nonparametric method in constructing the empirical and copula-based distributions can be found in Genest and Rivest (1993). The performance of each copula, shown in Table 1, is assessed based on the obtained p values from the Cramér-von Mises test. If the p value of the given copula is less than a specific significance level (e.g., 3%), the copula form is rejected. Therefore, high p values indicate the suitability of the copula form.

3.3. Constructing FDC by Combining FFDC and SFDC

Since the joint cumulative distribution function of fast flow and slow flow is quantified by the identified form of copula (equation (7)), equation (2) can be expressed as

$$F_{\boldsymbol{Q}}(q)=P\left(\boldsymbol{Q_f}+\boldsymbol{Q_s}\le q\right)=\iint_{\left\{\boldsymbol{Q_f}+\boldsymbol{Q_s}\le q\right\}}\mathrm{d}C\left(F_{\boldsymbol{Q}_f}\left(q_f\right),F_{\boldsymbol{Q}_s}(q_s)\right) \tag{9}$$

For a given value of $Q = q$, the value of $F_{\boldsymbol{Q}}(q)$ is the joint probability of fast flow and slow flow over the shaded area shown in Figure 2a, where $Q_{f,\min}$ and $Q_{s,\min}$ are the minimum values of fast flow and slow flow, respectively. $Q_{f,\min}$ is zero for all the case study catchments. As a property of copulas, the joint distribution of fast flow and slow flow over any rectangular area can be computed by the following equation (Nelsen, 2007):

10.1029/2019WR026083

Table 1
Three Archimedean Copulas and Their Formula for Estimating the Dependence Structure Between Fast Flow and Slow Flow

Family	$C\left(\left(F_{Q_f}\left(q_f\right), F_{Q_s}(q_s)\right)\right)$	Range of θ	Kendall's τ	Range of τ
Gumbel	$\exp\left[-\left[\left(-\ln\left(F_{Q_f}\left(q_f\right)\right)\right)^{\theta}+\left(-\ln\left(F_{Q_s}(q_s)\right)\right)^{\theta}\right]^{\frac{1}{\theta}}\right]$	$[1, \infty)$	$1-\theta^{-1}$	$[0,1]$
Clayton	$\left[\left(F_{Q_f}\left(q_f\right)\right)^{-\theta}+\left(F_{Q_s}(q_s)\right)^{-\theta}-1\right]^{-\frac{1}{\theta}}$	$[1, \infty)$	$\frac{\theta}{\theta+2}$	$[0.3,1]$
Frank	$\frac{1}{\theta}\ln\left[1+\frac{\left(\exp\left(\theta\cdot F_{Q_f}\left(q_f\right)\right)-1\right)\left(\exp\left(\theta\cdot F_{Q_s}(q_s)\right)-1\right)}{\exp(\theta)-1}\right]$	$(-\infty, 0)\cup(0,\infty)$	$1-\frac{4}{\theta}[D_1(-\theta)-1]$	$[-1,0)\cup(0,1]$

Note. Here D_1 is the first Debye function defined as $D_1(x)=\frac{1}{x}\int_0^x\frac{t}{e^t-1}dt$.

$$P\left(Q_f\epsilon\left(q_{f,l}, q_{f,u}\right], Q_s\epsilon\left(q_{s,l}, q_{s,u}\right]\right) = C\left(F_{Q_f}\left(q_{f,u}\right), F_{Q_s}\left(q_{s,u}\right)\right)-C\left(F_{Q_f}\left(q_{f,l}\right), F_{Q_s}\left(q_{s,u}\right)\right)-C\left(F_{Q_f}\left(q_{f,u}\right), F_{Q_s}\left(q_{s,l}\right)\right) +C\left(F_{Q_f}\left(q_{f,l}\right), F_{Q_s}\left(q_{s,l}\right)\right) \tag{10}$$

where $q_{f,l}$ and $q_{f,u}$ are the lower and upper bounds of fast flow for the rectangular area; and $q_{s,l}$ and $q_{s,u}$ are the lower and upper bounds of slow flow for the rectangular area.

Based on equation (10), a fast numerical algorithm was used to evaluate equation (9) by discretizing the shaded triangular area into rectangular areas as shown in Figure 2b (Embrechts & Puccetti, 2007). At the first iteration ($i = 1$), there is one rectangle, and the coordinates for the four corners of the rectangle in clockwise direction are ($Q_{f,\min}$, $Q_{s,\min}$), ($Q_{f,\min}$, $\frac{q-Q_{f,\min}+Q_{s,\min}}{2}$), ($\frac{q-Q_{s,\min}+Q_{f,\min}}{2}$, $\frac{q-Q_{f,\min}+Q_{s,\min}}{2}$), and ($\frac{q-Q_{s,\min}+Q_{f,\min}}{2}$, $Q_{s,\min}$). The joint probability of fast flow and slow flow over this rectangular area is computed from equation (10) by setting $q_{f,l} = Q_{f,\min}$, $q_{f,u} = \frac{q-Q_{s,\min}+Q_{f,\min}}{2}$, $q_{s,l} = Q_{s,\min}$, and $q_{s,u} = \frac{q-Q_{f,\min}+Q_{s,\min}}{2}$. There are two rectangles at the second iteration ($i = 2$), and there are four rectangles at the third iteration ($i = 3$) as shown in Figure 2b. Therefore, the number of added rectangles is 2^{i-1} at the ith iteration. The joint probability of fast flow and slow flow over each rectangular area is computed using equation (10) by substituting the corresponding coordinates of the corners of the rectangle. Since the probability over the rectangles decreases with increasing i, the joint probability of fast flow and slow flow over the shaded area in Figure 2a can be approximated by the sum of the joint probabilities over all the rectangles when the number of iteration is large enough. In this paper, the maximum number of iterations is set to 10 since root-mean-square error (RMSE) decreases

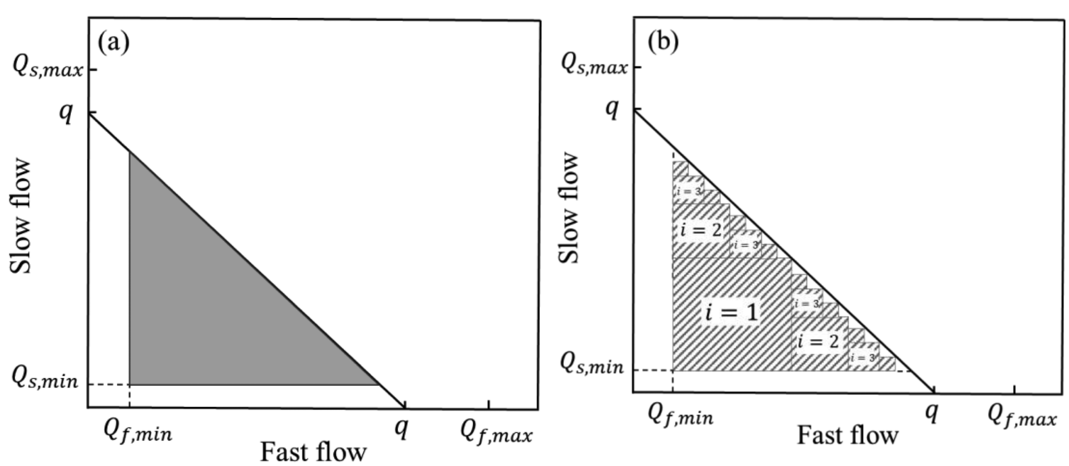

Figure 2. Demonstration of numerical computation of the CDF of streamflow (i.e., $F_Q(q)$). (a) The joint probability of fast flow and slow flow over the shaded area representing $F_Q(q)$; and (b) the discretization of the shaded area in (a) into infinite number of rectangles.

10.1029/2019WR026083

95% from the first iteration to the tenth iteration but the decrease in RMSE is less than 0.01% from the tenth iteration to the eleventh iteration. The computational time of aforementioned method in computing the CDF of streamflow is within seconds, which is much less than for other numerical methods such as Monte Carlo simulations.

It should be noted that Figure 2b only shows the case when $q \leq Q_{f,\max}+Q_{s,\min}$ and $q \leq Q_{s,\max}+Q_{f,\min}$ where $Q_{s,\max}$ and $Q_{f,\max}$ are maximum slow flow and fast flow, respectively. There are three more cases: (1) $q > Q_{f,\max}+Q_{s,\min}$ and $q > Q_{s,\max}+Q_{f,\min}$; (2) $q \geq Q_{f,\max}+Q_{s,\min}$ and $q < Q_{s,\max}+Q_{f,\min}$; and (3) $q < Q_{f,\max}+Q_{s,\min}$ and $q \geq Q_{s,\max}+Q_{f,\min}$. The calculation of $F_Q(q)$ for these three cases was performed in a similar way as in Figure 2a.

4. Results and Discussion

4.1. Baseflow Separation

For the process-based baseflow separation method (Wittenberg, 1999) the parameters are determined by the least squares method (Brooks et al., 2011; Sivapalan et al., 2011). For the filter-based method (Eckhardt, 2005) the two parameters are set as constants for all the catchments, that is, 0.98 for the recession constant and 0.8 for the upper bound of BFI (Eckhardt, 2005). The calculated BFI values for the study catchments range from 0.32 to 0.79 for the filter-based and from 0.25 to 0.94 for the process-based method. The filter-based method tends to give higher values of BFI than the process-based method when BFI is small, but lower values when it is large. However, as shown in Figure 3a, the BFI values obtained from these two methods match well in most catchments (R^2=0.95). Analysis of modeling the FDC as the sum of FFDC and SFDC is conducted based on the baseflow separation results from both methods, but results were found to be similar. Therefore, the results from the process-based separation are discussed in the following sections.

4.2. Construction of FDC by Convolution of FFDC and SFDC

Making the initial assumption that fast flow and slow flow are independent, the FDCs for the study catchments are constructed using a convolution between empirical FFDC and SFDC. The RMSE is computed to evaluate the performance of the independence assumption between daily fast flow and slow flow. In order to compute the RMSE, the maximum exceedance probability ($EP_{\max}$), which is determined by nonzero flows, is discretized into 1,000 quantiles, and the daily observed streamflow in each quantile is compared with the convolution-based streamflow at the same quantile. Figure 4 shows the computed RMSE between constructed and observed FDCs for the study catchments. The RMSE ranges from 0 to 2 (mm/day) for these catchments. For most catchments where RMSE is low, the convolution-based FDC matches the observed one well, and the FFDC and SFDC can be assumed to be relatively independent. Figures 5b, 5d, and 5f compare the convolution-based FDC and observed FDC in three catchments. For the Yadkin River in North Carolina the convolution works well with RMSE of 0.12 mm/day (Figure 5b), but for the Holston River in Virginia and the Satilla River in Georgia it is less accurate with RMSE of 0.27 mm/day (Figure 5d) and 0.32 mm/day (Figure 5f). It is clear that in these catchments, the dependence structure between fast flow and slow flow needs to be captured for constructing FDC.

4.3. Construction of FDC Considering the Dependency of FFDC and SFDC

4.3.1. Dependence Structure of FFDC and SFDC

In this section the dependence structure of FFDC and SFDC is quantified by the Kendall's τ shown in Table 1 . Figure 3b compares the values of Kendall's τ based on two baseflow separation methods used in this study. As can be seen, the values of τ from the process-based and filter-based separation methods are well correlated, and the difference of τ between the two methods is larger than that of BFI. However, the discussion related to the dependence is very similar for these two baseflow separation methods.

The spatial variation of estimated τ based on the process-based baseflow separation method over the study catchments indicates that the level of dependency between fast flow and slow flow has a regional pattern. For example, from Figure 6a, it can be seen that most catchments in northeastern United States (e.g., from Main to Ohio) have relatively higher values of τ (i.e., 0.25 in average), indicating a higher dependency between fast flow and slow flow. The northeastern catchments are classified as small catchments (i.e., 2,000 km^2 in average) with long and frequent storms and high fraction of snow days and with a high fraction of sand (i.e., 50% in average) (Sawicz et al., 2011). The high soil permeability, frequent storms, and high

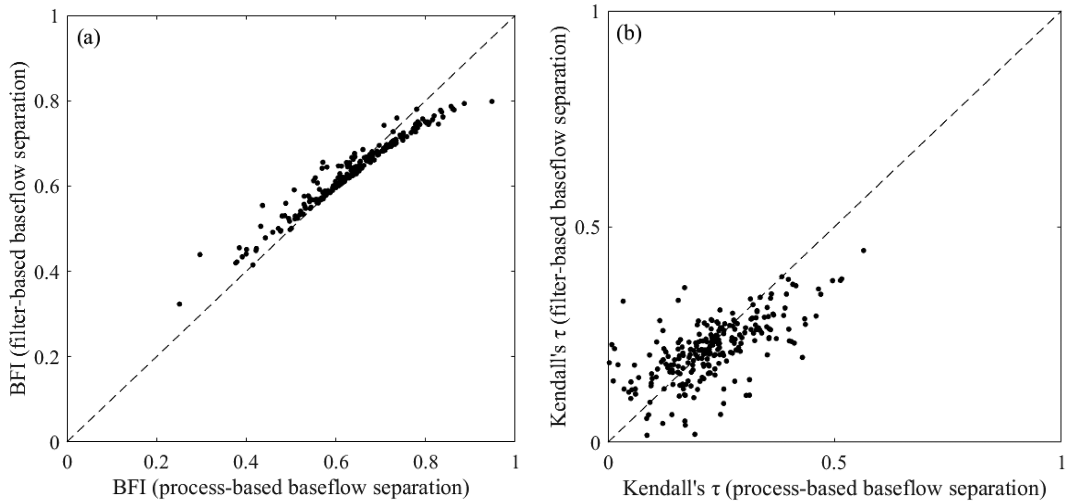

Figure 3. Comparison between two baseflow separation methods: process-based (Wittenberg, 1999) and filter-based (Eckhardt, 2005) in terms of (a) baseflow index (BFI) and (b) dependency between fast flow and slow flow components (Kendall's τ) over the study catchments.

fraction of snow days can increase the contribution of slow flow; on the other hand, the short time of concentration in small catchments can increase the contribution of fast flow, which results in the high potential for dependence between fast flow and slow flow in these catchments.

The controls of climate characteristics (e.g., climate aridity index, seasonality index (Walsh & Lawler, 1981), and time interval between storms) and catchment properties (e.g., drainage area, mean slope, and mean elevation) on the Kendall's τ are assessed over the study catchments. The catchment properties do not show significant controls on the Kendall's τ but climate characteristics show significant controls on the Kendall's τ (Figure 6).

From Figure 6b, it can be seen that there is no correlation between climatic aridity index (AI) and τ in humid regions (AI < 1), however, τ increases with AI in arid regions (AI > 1). Precipitation is the main controlling

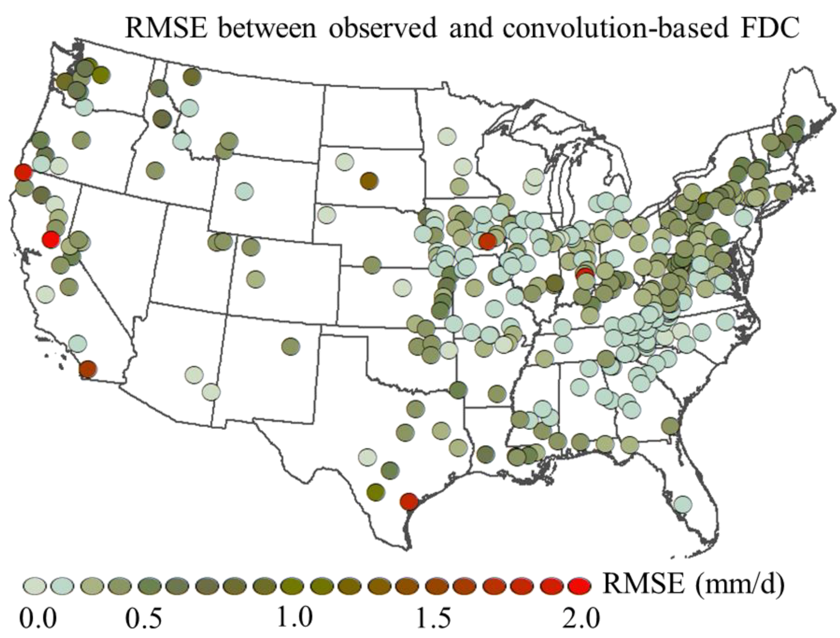

Figure 4. RMSE between observed FDC and constructed FDC using convolution between empirical FFDC and SFDC over the study catchments.

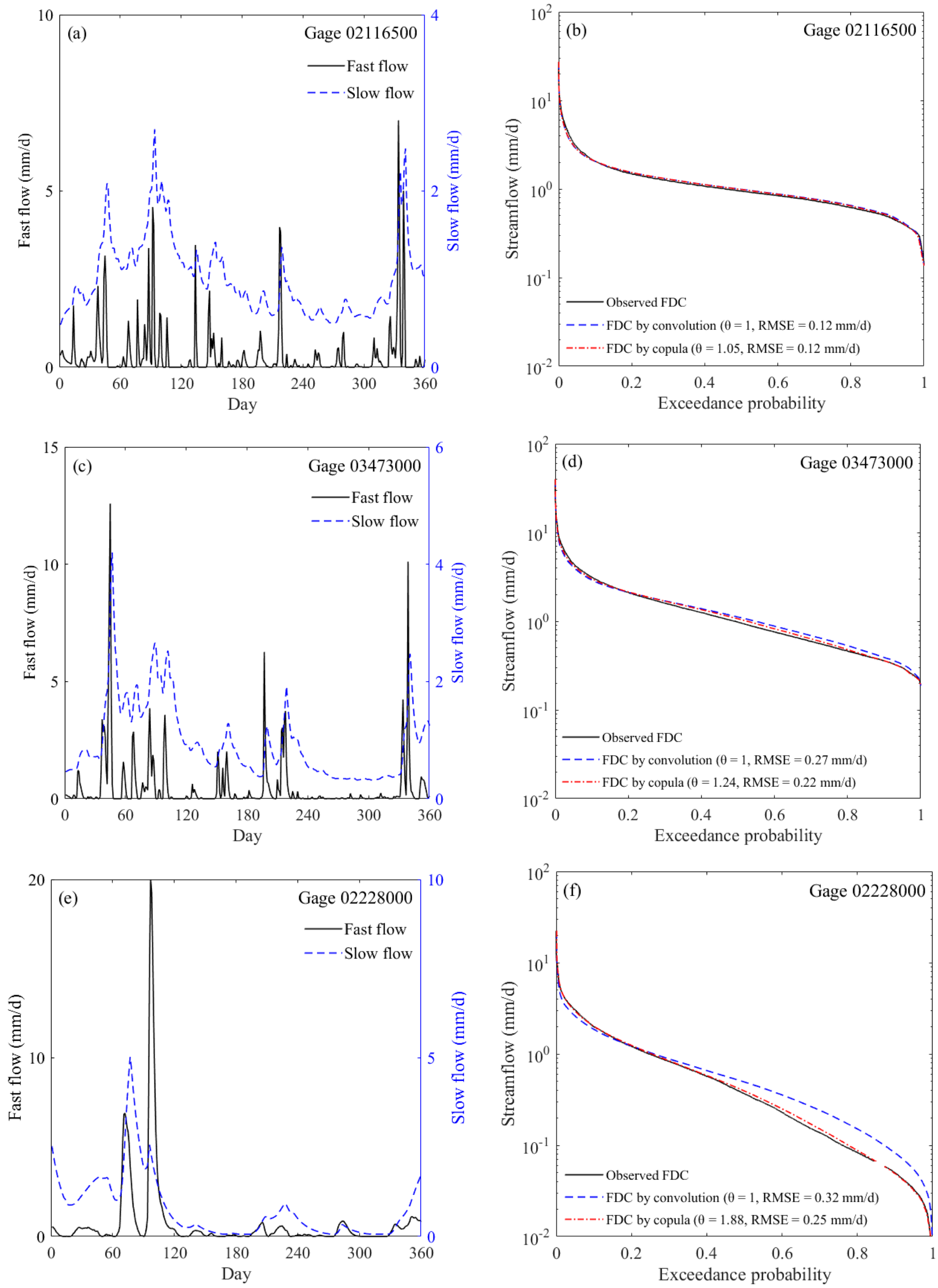

Figure 5. The fast flow and slow flow time series during 1 year and streamflow duration curve for the Yadkin River in North Carolina (a, b), the Holston River in Virginia (c, d), and the Satilla River in Georgia (e, f).

factor on fast flow in both humid and arid regions. In arid regions where water is limited, slow flow is also dominantly controlled by precipitation dynamics. Therefore, both fast flow and slow flow are controlled by precipitation in arid regions leading to the higher dependence of Kendall's τ on AI in drier catchments. However, in humid regions where energy is limited, potential evaporation plays an important role on slow

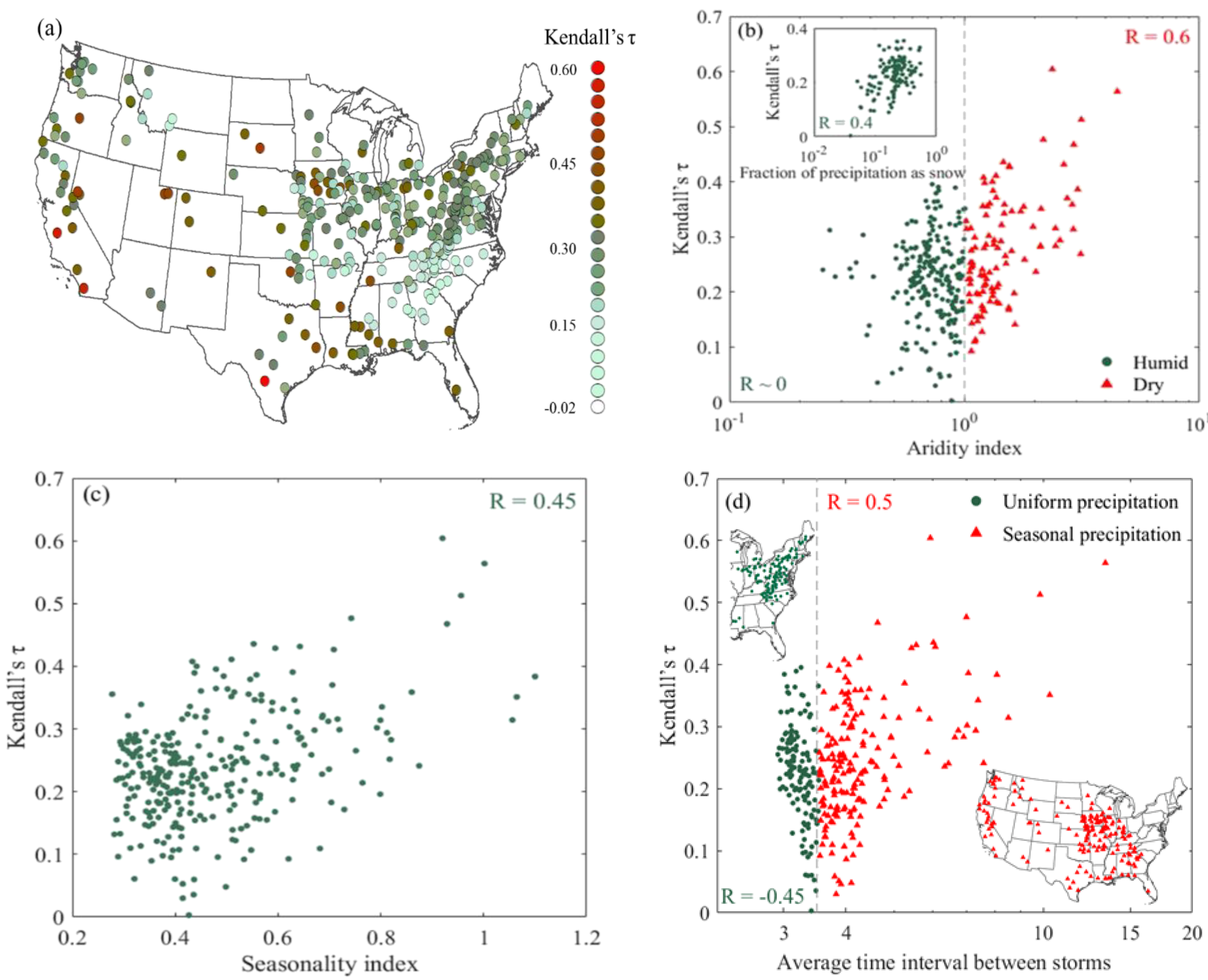

Figure 6. (a) The spatial distribution of the Kendall's τ and controls of Kendall's τ by the (b) aridity index, (c) seasonality index, and (d) average time interval between storms over the study catchments.

flow but not on fast flow, which leads to the lack of correlation between AI and Kendall's τ. In humid regions, the Kendall's τ based on the dominant processes is controlled by other indicators. For example, in the Pacific Northwest and northeastern parts of United States which are characterized by significant amount of snow, the snowiness is a potential factor controlling the Kendall's τ. The snowiness is defined as the fraction of precipitation falling as snow (Berghuijs et al., 2014). The increase of snowiness leads to increase of snow accumulation during the winter period, which contributes to a delay in generation of both fast flow and slow flow. The positive correlation between Kendall's τ and snowiness shown in the inset of Figure 6b arises from the coincidence of fast flow and slow flow generation during late spring.

The seasonality of precipitation, quantified by seasonality index (SI), also controls Kendall's τ. As can be seen in Figure 6c, there is a positive correlation between Kendall's τ and SI. The seasonality of fast flow is mainly controlled by the seasonality of precipitation as the main controlling factor on fast flow, whereas the seasonality of slow flow is controlled by the seasonality in precipitation, evaporation, and soil moisture content. For example, in regions with low seasonality in precipitation (i.e., low SI), a smaller variation in fast flow but a larger seasonal variation in slow flow is expected. The different seasonal variations in fast flow and slow flow for catchments with lower SI leads to the lower dependency between fast flow and slow flow.

Figure 6d provides more insights into the effect of rainfall variability on the Kendall's τ. The average time interval between storms (T_b) is computed to quantify the storminess characteristics in the study catchments. The average time-interval between storms is computed as the time elapsed between end of the storm and the

10.1029/2019WR026083

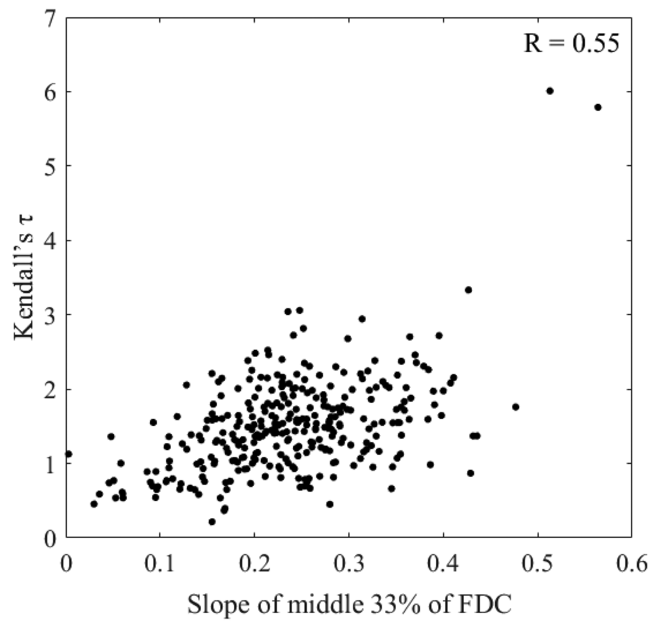

Figure 7. The correlation between slope of the middle 33% of FDC and the strength of dependence between fast flow and slow flow (i.e., Kendall's τ) over the study catchments.

beginning of the next storm based on the daily precipitation (Eagleson, 1978). From Figure 6d, it can be seen that there is a negative correlation between T_b and τ in northeastern United States where precipitation is distributed more uniformly throughout the year. The increase of T_b in this region contributes to increasing variability of soil water storage and subsequently increasing variability of slow flow. Therefore, the difference of variability in fast flow and slow flow, which arises from higher T_b, leads to decreasing Kendall's τ. However, the Kendall's τ in regions with seasonal precipitation increases with T_b, which is similar to the relation between Kendall's τ and AI.

The scatter plots shown in Figure 6 can be interpreted as the coevolution of different parameters in controlling the dependence of fast flow and slow flow. Moreover, the significance test for the Pearson correlation coefficient verified the identified relation at the significance level of 5%.

Figure 7 shows the control of Kendall's τ on the slope of empirical FDC over the exceedance probability range of 33–67%, which is linear on the semilog plot (Yadav et al., 2007). The slope of FDC in the middle part is mainly controlled by the SFDC, but it can also reflect the daily streamflow variability caused by FFDC (Castellarin et al., 2013; Yokoo & Sivapalan, 2011). For example, catchments with a dominance of slow flows have flatter slope of FDC; while the steeper slope of FDC shows the increase of variability in streamflow due to increasing fast flow contribution (Castellarin et al., 2013; Cheng et al., 2012; Lane & Lei, 1950; Sauquet & Catalogne, 2011; Sawicz et al., 2011). This is consistent with the identified positive correlation between Kendall's τ and the slope of FDC shown in Figure 7. In catchments with steeper slope of FDC, fast flow besides slow flow plays a role on controlling the middle part of FDC, leading to higher Kendall's τ; and in catchments with flatter slope, fast flow does not control the middle part of FDC causing lower Kendall's τ.

4.3.2. Construction of FDC by Combining FFDC and SFDC

The three copulas shown in Table 1 are applied to fast flow and slow flow in the study catchments. The p values of the Cramér-von Mises test exceed 3% for the Clayton copula in 180 catchments, for the Frank copula in 200 catchments, and for the Gumbel copula in 245 catchments, indicating the suitability of these three copulas at the confidence level of 97% in the corresponding catchments. There are 27 catchments for which the three copulas are not able to capture the joint distributions. For the catchments where these three Archimedean copulas cannot capture the dependency between fast flow and slow flow, other copulas need to be explored. However, one potential reason can be the existence of strong autocorrelation in fast and slow flow time series. For those catchments with strong autocorrelation, the time series of fast flow and slow flow can be modeled as the linear combination of autoregressive (AR), moving average (MA), and residual error

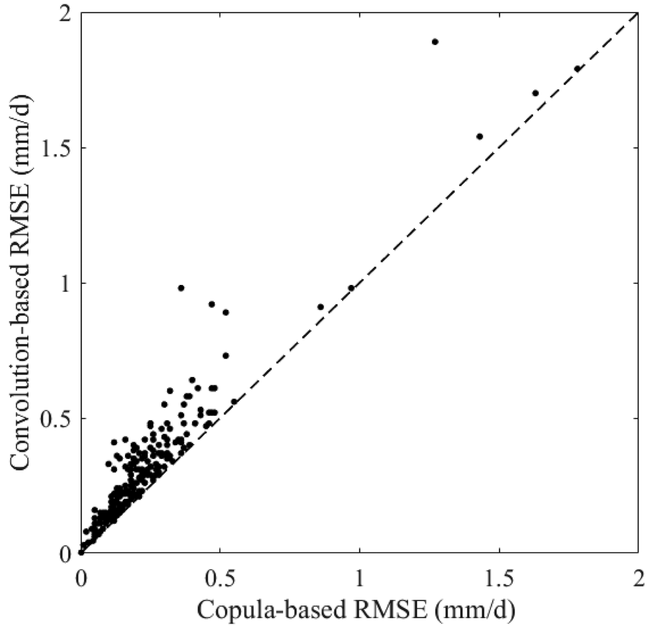

Figure 8. Comparison of RMSE of constructed FDC between the convolution-based method (without dependency) and the copula-based method (accounting for dependency) over 245 catchments.

terms. The FDC is modeled as the summation of the corresponding terms of fast and slow flows in terms of ARMA, which has less autocorrelation compared with the original time series and residual error term, which are white noise with Gaussian distribution (Hofert et al., 2018; Zhang & Singh, 2019). The application of the proposed framework on the modeled time series of fast flow and slow flow is beyond the scope of this paper. For consistency, the Gumbel copula is selected for modeling the joint distribution of fast flow and slow flow for all 245 catchments.

In the Gumbel copula, $\theta = 1$ indicates that fast flow and slow flow are independent, and $\theta > 1$ indicates positive dependency. Figure 5 shows the daily variation of fast flow and slow flow in three catchments with different levels of dependency, i.e., perfect independence, mild dependence, and strong dependence. For example, θ for the Yadkin River in North Carolina is 1.05 which indicates almost perfect independence (Figure 5a), and the Holston River in Virginia has a mild dependence with $\theta = 1.24$ (Figure 5c). The Satilla River in Georgia, where both fast flow and slow flow vary seasonally, has a strong dependency with $\theta = 1.88$ (Figure 5e).

The computed FDCs with and without accounting for dependency is compared with the observed FDC in three stations with different levels of dependence (Figures 5b, 5d, and 5f). For the Yadkin River (Figure 5b), both the convolution-based FDC (equation (6)) and copula-based FDC (equation (9)) match the observed FDC well because fast flow and slow flow are almost independent ($\theta = 1.05$). Therefore, for the catchments with θ close to 1 (e.g., Appalachian Mountain), FDC can be directly computed as the convolution of FFDC and SFDC. However, Figure 5f shows significant errors in convolution-based FDC for the Satilla River in Georgia (RMSE = 0.32 mm/day) where θ is 1.88. The copula-based FDC has a better performance (RMSE = 0.25 mm/day) than the convolution-based FDC and in particular fits the low flows much better. For catchments with high values of θ (e.g., Southern California and Middle Iowa), the cross-dependence of fast and slow flows needs to be captured for modeling FDC. Figure 8 compares the RMSE for the convolution-based and copula-based FDCs over the 245 catchments. As shown in Figure 8, the copula-based FDC always has a smaller RMSE than the convolution-based FDC, especially when RMSE is higher (i.e., higher value of θ).

The performance of the proposed framework for constructing FDC is also assessed by the goodness-of-fit measure using the Cramér-von Mises test. The high p value over 245 catchments (i.e., 0.2 in average) represents that the constructed FDC using the Gumbel copula is consistent with the empirical FDC at the significance level of 0.05.

As the purpose of this paper is limited to illustrating the new conceptual framework for studying FDC by combining FFDC and SFDC, we applied the framework using empirically derived FFDCs and SFDC instead of modeled ones. Process-based models for FFDC and SFDC could be developed, and the FDC could then be constructed as their sum using the proposed framework.

5. Conclusions

The FDC represents the variability of daily streamflow in the probability domain at different time scales, including quick response to storminess and a slow response to climate seasonality (Pumo et al., 2013; Yokoo & Sivapalan, 2011). Guided by this consideration, in this study we presented a new framework for understanding process controls of FDCs, which involves separating total streamflow into a fast and a slow component. The FDC is constructed by combing FDCs of fast and slow flows (i.e., FFDC and SFDC, respectively) and a measure of their dependency.

We quantified the dependence structure between fast flow and slow flow by the Kendall's τ. There are regional patterns of the dependence between fast flow and slow flow which can be explained by climate characteristics and catchment properties. In catchments where the dependence is small, the FDC can simply be constructed by a convolution of the duration curves of fast flows and slow flows, while in the catchments with strong dependence it is essential to construct the FDC by accounting for this dependence. The study explored the climatic and landscape controls on the dependence between FFDC and SFDC. This comparison indicates that the control of climate characteristics on the dependency is more significant than landscape properties. Further research needs to be conducted to obtain more insight into the hydrologic controls on the dependence structure of fast and slow flows.

We compared three Archimedean copulas (i.e., Gumbel, Clayton, and Frank) and found that the Gumbel copula can capture the joint distribution of fast flow and slow flow well for most of the study catchments. Application of Gumbel copula in 245 catchments, demonstrates the validity of the proposed framework in constructing the FDC by combining FFDC and SFDC at the significance level of 5%.

The goal of this paper is to demonstrate the feasibility of the framework; process-based modeling of FFDC and SFDC, and their dependency, is not the focus, which will be reported in the future. The framework proposed in this paper provides a tool for linking the fast flow and slow flow components, which are controlled by processes on two different time scales. In this way it allows attributing the shape of the flow duration curve to the physical processes and provides an avenue for predicting FDCs in ungagged basins. The framework can also be applied for constructing AFDCs from annual fast flow duration curve and annual slow flow duration curve.

Appendix A.: Baseflow Separation Methods

A.1. Process-Based Separation Method

The processed-based method is based on the nonlinear storage-outflow relationship:

$$S = aQ_s{}^b \qquad \text{and} \qquad Q_s = -\frac{\mathrm{d}S}{\mathrm{d}t} \tag{A1}$$

where S (m^3) is the volume of stored water in the aquifer; Q_s (m^3/s) is slow flow; and a (m$^{3\text{-}3b}$s^b) and b (dimensionless) are the catchment properties. Solving equation (A1) for the slow flow, the recession equation is obtained as

$$Q_s(t-\Delta t) = \left[Q_s(t)^{b-1} + \frac{(b-1)\Delta t}{ab}\right]^{1/(b-1)} \tag{A2}$$

The time step Δt is normally 1 day. The parameters of a and b are estimated by fitting equation (A2) to the observed recessions in each catchment. The recession limb is constructed by starting from the last value of the streamflow time series and proceeding backward over t to compute slow flow at $t - \Delta t$. The peak of slow flow is determined based on the intersection point of slow flow recession limb and streamflow rising limb. One time step forward from the intersection point shows the peak of slow flow. The rising limb of slow flow is computed in a similar way to the recession limb calculation for one time step forward for each streamflow value.

A.2. Filter-Based Separation Method

The filter-based method is based on the separation of low-frequency signals (slow flow) from high-frequency signals (fast flow). The slow flow from the filter based is computed as

$$Q_s(t) = \frac{(1-BFI_{\max})\alpha Q_s(t-1) + (1-\alpha)BFI_{\max}Q(t)}{1-\alpha BFI_{\max}} \tag{A3}$$

where $Q(t)$ is the streamflow at t; $Q_s(t-1)$ is the filtered slow flow at $t - 1$; α is the filter parameter ($0 < \alpha < 1$); and $BFI_{\max}$ is the upper bound of baseflow index. The filter-based separation can be performed using the Web-based Hydrograph Analysis Tool (Lim et al., 2005).

Acknowledgments

This research was funded in part under Award CBET-1804770 from National Science Foundation. The MOPEX data set used to complete the analysis in this paper are downloaded from this site (ftp://hydrology.nws.noaa.gov/pub/gcip/mopex/US_Data/). The authors thank Riccardo Rigon and three anonymous reviewers for their constructive comments and suggestions, which have led to substantial improvements over an earlier version of the paper.

References

Beckers, J., & Alila, Y. (2004). A model of rapid preferential hillslope runoff contributions to peak flow generation in a temperate rain forest watershed. *Water Resources Research*, *40*, W03501. https://doi.org/10.1029/2003WR002582

Berghuijs, W. R., Sivapalan, M., Woods, R. A., & Savenije, H. H. G. (2014). Patterns of similarity of seasonal water balances: A window into streamflow variability over a range of time scales. *Water Resources Research*, *50*, 5638–5661. https://doi.org/10.1002/2014WR015692

Best, A. E., Zhang, L., McMahon, T. A., & Western, A. W. (2003). Development of a model for predicting the changes in flow duration curves due to altered land use conditions, presented at MODSIM 2003, Townsville, 14-17 July, pp. 861-866.

Blöschl, G., Sivapalan, M., Wagener, T., Viglione, A., & Savenije, H. H. G. (Eds.) (2013). *Runoff predictions in ungauged basins: A synthesis across processes, places and scales*. Cambridge: Cambridge University Press.

Botter, G., Porporato, A., Daly, E., Rodriguez-Iturbe, I., & Rinaldo, A. (2007). Probabilistic characterization of base flows in river basins: Roles of soil, vegetation, and geomorphology. *Water Resources Research*, *43*, W06404. https://doi.org/10.1029/2006WR005397

Botter, G., Porporato, A., Rodriguez-Iturbe, I., & Rinaldo, A. (2007). Basin scale soil moisture dynamics and the probabilistic characterization of carrier hydrologic flows: Slow, leaching prone components of the hydrologic response. *Water Resources Research*, *43*, W02417. https://doi.org/10.1029/2006WR005043

Botter, G., Porporato, A., Rodriguez-Iturbe, I., & Rinaldo, A. (2009). Nonlinear storage-discharge relations and catchment streamflow regimes. *Water Resources Research*, *45*, W10427. https://doi.org/10.1029/2008WR007658

Brooks, P. D., Troch, P. A., Durcik, M., Gallo, E., & Schlegel, M. (2011). Quantifying regional scale ecosystem response to changes in precipitation: Not all rain is created equal. *Water Resources Research*, *47*, W00J08. https://doi.org/10.1029/2010WR009762

Castellarin, A., Botter, G., Hughes, D. A., Liu, S., Ouarda, T. B. M. J., Parajka, J., et al. (2013). Prediction of flow duration curves in ungauged basins. In G. Blöschl, et al. (Eds.), *Runoff prediction in ungauged basins, synthesis across processes, places and scales* (Chap. 7, pp. 135–162). Cambridge, UK: Cambridge University Press.

Castellarin, A., Camorani, G., & Brath, A. (2007). Predicting annual and long-term flow-duration curves in ungauged basins. *Advances in Water Resources*, *30*(4), 937–953. https://doi.org/10.1016/j.advwatres.2006.08.006

Castellarin, A., Vogel, R. M., & Brath, A. (2004). A stochastic index flow model of flow duration curves. *Water Resources Research*, *40*, W03104. https://doi.org/10.1029/2003WR002524

Chen, X., Fan, Y., & Patton, A. J. (2004) Simple tests for models of dependence between multiple financial time series, with applications to U.S. equity returns and exchange rates. *London Economics Financial Markets Group working paper*, 483.

Cheng, L., Yaeger, M., Viglione, A., Coopersmith, E., Ye, S., & Sivapalan, M. (2012). Exploring the physical controls of regional patterns of flow duration curves. Part 1: Insights from statistical analyses. *Hydrology and Earth System Sciences*, *16*(11), 4435–4446. https://doi.org/10.5194/hess-16-4435-2012

Dingman, S. L. (1981). Planning level estimates of the value of reservoirs for water supply and flow augmentation in New Hampshire. *Water Resources Bulletin*, *17*(8), 684–690. https://doi.org/10.1111/j.1752-1688.1981.tb01277.x

Duan, Q., Schaake, J., Andréassian, V., Franks, S., Goteti, G., Gupta, H. V., et al. (2006). Model parameter estimation experiment (MOPEX): An overview of science strategy and major results from the second and third workshops. *Journal of Hydrology*, *320*(1-2), 3–17. https://doi.org/10.1016/j.jhydrol.2005.07.031

Eagleson, P. S. (1978). Climate, soil, and vegetation: 2. The distribution of annual precipitation derived from observed storm sequences. *Water Resources Research*, *14*(5), 713–721. https://doi.org/10.1029/WR014i005p00713

Eckhardt, K. (2005). How to construct recursive digital filters for baseflow separation. *Hydrological Processes*, *19*(2), 507–515. https://doi.org/10.1002/hyp.5675

Embrechts, P., & Puccetti, G. (2007). Fast computation of the distribution of the sum of two dependent random variables. *Preprint to Elsevier*.

Favre, A. C., El Adlouni, S., Perreault, L., Thiemonge, N., & Bobee, B. (2004). Multivariate hydrological frequency analysis using copulas. *Water Resources Research*, *40*, W01101. https://doi.org/10.1029/2003WR002456

Fermanian, J. D. (2005). Goodness-of-fit tests for copulas. *Journal of Multivariate Analysis*, *95*(1), 119–152. https://doi.org/10.1016/j.jmva.2004.07.004

Genest, C., & MacKay, R. J. (1986). The joy of copulas: Bivariate distributions with uniform marginals. *The American Statistician*, *40*(4), 280–283. https://doi.org/10.2307/2684602

Genest, C., Quessy, J. F., & Rémillard, B. (2006). Goodness-of-fit procedures for copula models based on the probability integral transformation. *Scandinavian Journal of Statistics*, *33*(2), 337–366. https://doi.org/10.1111/j.1467-9469.2006.00470.x

Genest, C., & Rémillard, B. (2008). Validity of the parametric bootstrap for goodness-of-fit testing in semiparametric models. *Annales de l'Institut Henri Poincare (B)*, *44*(6), 1096–1127. https://doi.org/10.1214/07-AIHP148

Genest, C., & Rivest, L. P. (1993). Statistical Inference Procedures for bivariate Archimedean copulas. *Journal of the American Statistical Association*, *88*(423), 1034–1043.

Grimaldi, S., & Serinaldi, F. (2006). Asymmetric copula in multivariate flood frequency analysis. *Advances in Water Resources*, *29*(8), 1155–1167. https://doi.org/10.1016/j.advwatres.2005.09.005

Hofert, M., Kojadinovic, I., Mächler, M., & Yan, J. (2018). *Elements of copula modeling with R*. Cham: Springer.

Horton, R. E. (1933). The role of infiltration in the hydrologic cycle. *Transactions AGU*, *14*(1), 446–460. https://doi.org/10.1029/TR014i001p00446

Kao, S. C., & Govindaraju, R. S. (2008). Trivariate statistical analysis of extreme rainfall events via the Plackett family of copulas. *Water Resources Research*, *44*, W02415. https://doi.org/10.1029/2007WR006261

Lane, E. W., & Lei, K. (1950). Streamflow variability. *Transactions of the American Society of Civil Engineers*, *115*(1), 1084–1134.

Lane, P. N. J., Best, A. E., Hickel, K., & Zhang, L. (2005). The response of flow duration curves to afforestation. *Journal of Hydrology*, *310*(1-4), 253–265. https://doi.org/10.1016/j.jhydrol.2005.01.006

Li, M., Shao, Q., Zhang, L., & Chiew, F. H. (2010). A new regionalization approach and its application to predict flow duration curve in ungauged basins. *Journal of Hydrology*, *389*, 137–145. https://doi.org/10.1016/j.jhydrol.2010.05.039L

Lim, K. J., Engel, B. A., Tang, Z., Choi, J., Kim, K. S., Muthukrishnan, S., & Tripathy, D. (2005). Automated web GIS based hydrograph analysis tool, WHAT. *Journal of the American Water Resources Association*, *41*(6), 1407–1416. https://doi.org/10.1111/j.1752-1688.2005.tb03808.x

10.1029/2019WR026083

Lyne, V., & Hollick, M. (1979). Stochastic time variable rainfall-runoff modelling. In *Hydrology and water resources symposium*, edited by Institute of Engineers Australia National Conference Publication (pp. 89–93). Perth: Institute of Engineers Australia.

Mohamoud, Y. M. (2008). Prediction of daily flow duration curves and streamflow for ungauged catchments using regional flow duration curves. *Hydrological Sciences Journal*, *53*(4), 706–724. https://doi.org/10.1623/hysj.53.4.706

Morrison, M. A., & Bonta, J. V. (2008). Development of duration-curve based methods for quantifying variability and change in watershed hydrology and water quality, U.S. Environmental Protection Agency.

Müller, M. F., Dralle, D. N., & Thompson, S. E. (2014). Analytical model for flow duration curves in seasonally dry climates. *Water Resources Research*, *50*, 5510–5531. https://doi.org/10.1002/2014WR015301

Neff, B. P., Day, S. M., Piggott, A. R., & Fuller, L. M. (2005). Base flow in the Great Lakes basin, U.S. Geological Survey.

Nelsen, R. B. (2007). *An introduction to copulas*. New York: Springer Science and Business Media.

Olden, J. D., & Poff, N. L. (2003). Toward a mechanistic understanding and prediction of biotic homogenization. *The American Naturalist*, *162*(4), 442–460. https://doi.org/10.1086/378212

Over, T. M., Farmer, W. H., & Russell, A. M. (2018). Refinement of a regression-based method for prediction of flow-duration curves of daily streamflow in the Conterminous United States, U.S. Department of the Interior, U.S. Geological Survey.

Poff, N. L., Allan, J., Bain, M. B., Karr, J. R., Pestegaard, K. L., Richter, B. D., et al. (1997). The natural flow regime: A paradigm for river conservation and restoration. *BioScience*, *47*(11), 769–784. https://doi.org/10.2307/1313099

Pumo, D., Noto, L. V., & Viola, F. (2013). Ecohydrological modelling of flow duration curve in Mediterranean river basins. *Advances in Water Resources*, *52*, 314–327. https://doi.org/10.1016/j.advwatres.2012.05.010

Salvadori, G., & De Michele, C. (2004). Frequency analysis via copulas: Theoretical aspects and applications to hydrological events. *Water Resources Research*, *40*, W12511. https://doi.org/10.1029/2004WR003133

Sauquet, E., & Catalogne, C. (2011). Comparison of catchment grouping methods for flow duration curve estimation at ungauged sites in France. *Hydrology and Earth System Sciences*, *15*, 2421–2435. https://doi.org/10.5194/hess-15-2421-2011

Sawicz, K., Wagener, T., Sivapalan, M., Troch, P. A., & Carrillo, G. (2011). Catchment classification: Empirical analysis of hydrologic similarity based on catchment function in the eastern USA. *Hydrology and Earth System Sciences*, *15*(9), 2895–2911. https://doi.org/10.5194/hess-15-2895-2011

Schweizer, B., & Wolff, E. F. (1981). On nonparametric measures of dependence for random variables. *The Annals of Statistics*, *9*(4), 879–885.

Searcy, J. K. (1959). Flow-duration curves, Manual of hydrology, U.S. Geological Survey.

Shiau, J. T. (2006). Fitting draught duration and severity with two dimensional copulas. *Water Resources Management*, *20*(5), 795–815. https://doi.org/10.1007/s11269-005-9008-9

Singh, K. P. (1971). Model flow duration and streamflow variability. *Water Resources Research*, *7*(4), 1031–1036. https://doi.org/10.1029/WR007i004p01031

Singh, R. D., Mishra, S. K., & Chowdhary, H. (2001). Regional flow duration models for large number of ungauged Himalayan catchments for planning microhydro projects. *Journal of Hydrologic Engineering*, *6*(4), 310–316. https://doi.org/10.1061/(ASCE)1084-0699(2001)6:4(310)

Sivapalan, M., Yaeger, M. A., Harman, C. J., Xu, X., & Troch, P. A. (2011). Functional model of water balance variability at the catchment scale: 1. Evidence of hydrologic similarity and space-time symmetry. *Water Resources Research*, *47*, W02522. https://doi.org/10.1029/2010WR009568

Sklar A. (1959), Fonctions de re´partition a` n dimensions et leurs marges, Pub. I. Stat., 8, 229-231.

Smakhtin, V. U. (2001). Low flow hydrology: A review. *Journal of Hydrology*, *240*(3-4), 147–186. https://doi.org/10.1016/s0022-1694(00)00340-1

Szolgay, J., Gaál, L., Bacigál, T., Kohnová, S., Hlavčová, K., Výleta, R., et al. (2016). A regional comparative analysis of empirical and theoretical flood peak-volume relationships. *Journal of Hydrology and Hydromechanics*, *64*(4), 367–381. https://doi.org/10.1515/johh-2016-0042

Vogel, R. M., & Fennessey, N. M. (1994). Flow duration curves. 1. New interpretation and confidence intervals. *Journal of Water Resources Planning and Management*, *120*(4), 485–504. https://doi.org/10.1061/(ASCE)0733-9496

Vogel, R. M., & Fennessey, N. M. (1995). Flow duration curve II: A review of applications in water resources planning. *Journal of the American Water Resources Association*, *31*(6), 1029–1039. https://doi.org/10.1111/j.1752-1688.1995.tb03419.x

Walsh, R. P. D., & Lawler, D. M. (1981). Rainfall seasonality: Description, spatial patterns and change through time. *Weather*, *36*(7), 201–208. https://doi.org/10.1002/j.1477-8696.1981.tb05400.x

Wang, D., & Hejazi, M. (2011). Quantifying the relative contribution of the climate and direct human impacts on mean annual streamflow in the contiguous United States. *Water Resources Research*, *47*, W00J12. https://doi.org/10.1029/2010WR010283

Wittenberg, H. (1999). Baseflow recession and recharge as nonlinear storage processes. *Hydrological Processes*, *13*(5), 715–726. https://doi.org/10.1002/(SICI)1099-1085(19990415)

Wittenberg, H., Aksoy, H., & Miegel, K. (2019). Fast response of groundwater to heavy rainfall. *Journal of Hydrology*, *571*, 837–842. https://doi.org/10.1016/j.jhydrol.2019.02.037

Wittenberg, H., & Sivapalan, M. (1999). Watershed groundwater balance estimation using streamflow recession analysis and baseflow separation. *Journal of Hydrology*, *219*(1), 20–33. https://doi.org/10.1016/S0022-1694(99)00040-2

Yadav, M., Wagener, T., & Gupta, H. (2007). Regionalization of constraints on expected watershed response for improved predictions in ungauged basins. *Advances in Water Resources*, *30*(8), 1756–1774. https://doi.org/10.1016/j.advwatres.2007.01.005

Yaeger, M. A., Coopersmith, E., Ye, S., Cheng, L., Viglione, A., & Sivapalan, M. (2012). Exploring the physical controls of regional patterns of flow duration curves—Part 4. A synthesis of empirical analysis, process modeling and catchment classification. *Hydrology and Earth System Sciences*, *16*(11), 4483–4498. https://doi.org/10.5194/hess-16-4483-2012

Ye, S., Yaeger, M., Coopersmith, E., Cheng, L., & Sivapalan, M. (2012). Exploring the physical controls of regional patterns of flow duration curves—Part 2: Role of seasonality, the regime curve, and associated process controls. *Hydrology and Earth System Sciences*, *16*(11), 4447–4465. https://doi.org/10.5194/hess-16-4447-2012

Yokoo, Y., & Sivapalan, M. (2011). Towards reconstruction of the flow duration curve: Development of a conceptual framework with a physical basis. *Hydrology and Earth System Sciences*, *15*(9), 2805–2819. https://doi.org/10.5194/hess-15-2805-2011

Zhang, L., & Singh, V. P. (2006). Bivariate flood frequency analysis using the copula method. *Journal of Hydrology*, *332*(1-2), 93–109. https://doi.org/10.1016/j.jhydrol.2006.06.033

Zhang, L., & Singh, V. P. (2007). Gumbel-Hougaard copula for trivariate rainfall frequency analysis. *Journal of Hydrologic Engineering*, *12*(4), 409–419. https://doi.org/10.1061/(ASCE)1084-0699(2007)12:4(409)

Zhang, L., & Singh, V. P. (2019). *Copulas and their applications in water resources engineering*. Cambridge: Cambridge University Press.